

Long-wavelength instabilities in a system of interacting active particles

Zahra Fazli

Department of Physics, Institute for Advanced Studies in Basic Sciences (IASBS),
Zanjan 45137-66731, Iran

Ali Najafi

Department of Physics, Institute for Advanced Studies in Basic Sciences (IASBS),
Zanjan 45137-66731, Iran

Research Center for Basic Sciences & Modern Technologies (RBST), Institute for
Advanced Studies in Basic Sciences (IASBS), Zanjan 45137-66731, Iran

E-mail: najafi@iasbs.ac.ir

Abstract. Based on a microscopic model, we develop a continuum description for a suspension of microscopic self propelled particles. With this continuum description we study the role of long-range interactions in destabilizing macroscopic ordered phases that are developed by short-range interactions. Long-wavelength fluctuations can destabilize both isotropic and also symmetry broken polar phase in a suspension of dipolar particles. The instabilities in a suspension of pullers (pushers) arise from splay (bend) fluctuations. Such instabilities are not seen in a suspension of quadrupolar particles.

PACS numbers: 05.10.Gg, 05.65.+b, 87.18.Gh, 47.63.mf

Keywords: active suspension, instability, non-equilibrium statistical mechanics, long-range interactions.

1. Introduction

Dynamics of a suspension of interacting active particles, as a non-equilibrium problem in statistical mechanics, has attracted enormous interests in recent years [1, 2, 3, 4]. Systems like schools of fishes and birds [5, 6, 7], bacterial colonies [8, 9, 10, 11], gels of bio-polymers [12] and interacting active Janus particles [13, 14, 15] show a wide range of fascinating physical behavior. Coherent collective motions, long-range orientational order, large number fluctuations and pattern formations are examples of such phenomena [8, 16, 17].

Existence of long-range order in two-dimensional active systems [17, 18] seems to be in contrast with Mermin-Wagner theorem at first glance. As a result of that theorem, true order in low dimensional equilibrium systems is not possible [19], but a theoretical work based on renormalization group analysis by Toner and Tu has revealed a physical scenario in which, non-equilibrium nature of active systems can provide conditions for true order in lower dimensions [20]. Usually, short-range interactions are responsible for developing ordered phases but the role of long-range interactions, needs to be considered carefully [21, 22, 23, 24]. In a system composed of active particles suspended in aqueous media, hydrodynamic interactions provide long-range forces that can propagate like $1/r^2$ to long distances. In systems with long-range interactions, macroscopic ordered phases developed by short-range interactions are under dynamical instabilities due to long-wavelength fluctuations [25, 26, 27, 28]. Such instabilities are very sensitive to microscopic details of swimming mechanisms that can distinguish a pusher, puller or a neutral swimmer [29, 30]. Studying such instabilities is the main purpose of current article.

In addition to numerical studies [31, 32, 33], continuum descriptions can provide analytical tools in dealing with such non-equilibrium systems. Microscopic derivations [34] and symmetry arguments [20] are two approaches that can provide the governing equations for macroscopic continuum fields. While a large amount of works are devoted to the symmetry based theories [35, 36, 37], less efforts are concentrated on microscopic derivations [21, 38].

In this article we aim to use a microscopic approach and obtain the equations of macroscopic description. The continuum description derived from a microscopic model in this article, will allow us to study the role of long-range interactions in instabilities observed in active suspensions. Theories based on symmetry arguments reveals qualitative features of the long-wavelength instabilities in active suspensions. Microscopic based models can help us to understand the origin of instabilities more quantitatively. We will show that both isotropic and polar phases that can appear in active systems are unstable with respect to long-wavelength fluctuations.

The structure of this article is as follows: In section 2, we present the hydrodynamic details of our microscopic model and introduce long- and short-range interactions between swimmers. Then in section 3, we describe the dynamics of a suspension of many swimmers in terms of Langevin and Smoluchowski descriptions. Furthermore, in

this section, we simplify the description by considering mean field approximation. In section 4, we derive a continuum description for the system. Dynamical equations, their steady state solutions and instability analysis are presented in this section. Finally, discussion and summary are presented in section 5.

2. Hydrodynamic model for micro-swimmers

We start with a microscopic model for a minimal autonomous micro-swimmer that can propel itself at aqueous media. Theoretical arguments based on symmetry grounds show that a minimum number of two internal degrees of freedom is necessary to capture the hydrodynamic details of a micro-swimmer [39]. To construct the model swimmer, consider three spheres with radii a , connected linearly by two arms with variable lengths given by L^f and L^b . We label the spheres by f (front), b (back) and m (middle). It is shown that harmonic changes in the arm lengths with a phase lag between arms, will result a non zero swimming velocity for this system [40, 41]. To see how the above swimmer can work, one needs to solve the hydrodynamic equations for the ambient fluid that are coupled to the motion of spheres. At the scale of micrometer with velocity range about micrometer per second in water, the linear Stokes equation governs the dynamics of the fluid. Assuming that the arms are thin enough to neglect their hydrodynamic effects and eliminating the fluid degrees of freedom, one can reach to effective equations that govern the dynamics of spheres alone. Such equations are linear relations between the velocity of spheres and hydrodynamic forces acting by spheres on the fluid [42]:

$$v_i^m = \sum_{j,n} O_{ij}^{mn} f_j^n, \quad (1)$$

where f_j^n (v_j^n) denotes the j -th component of the force (velocity) of sphere n and the details of the hydrodynamic interactions are given by the kernel O_{ij}^{mn} . This hydrodynamic kernel is a function of the size of spheres and their relative position. Denoting the distance between spheres m and n by $\mathbf{d} = \mathbf{x}^m - \mathbf{x}^n$ and fluid viscosity by η and in the limit of $d \gg a$, Oseen's tensor provides an approximation for the hydrodynamic kernel [42]:

$$O_{ij}^{mn} = \begin{cases} \frac{1}{8\pi\eta d} (\delta_{ij} + \hat{d}_i \hat{d}_j) & \text{for } m \neq n \\ \frac{\delta_{ij}}{6\pi\eta a} & \text{for } m = n \end{cases}. \quad (2)$$

As the swimmer is autonomous, one needs to add the conditions of zero total force and zero total torque to the above dynamical equations. The above relations and the constraints that prescribe the dynamics of arm lengths provide a complete set of dynamical equations that can fully determine the state of the swimmer, including its speed, direction and forces. Velocities and forces averaged over time, are the quantities that we are interested to know. To express the results, let us assume that the arms oscillate around a mean value ℓ as:

$$L^f(t) = \ell + u^f(t), \quad L^b(t) = \ell(1 + \delta) + u^b(t), \quad (3)$$

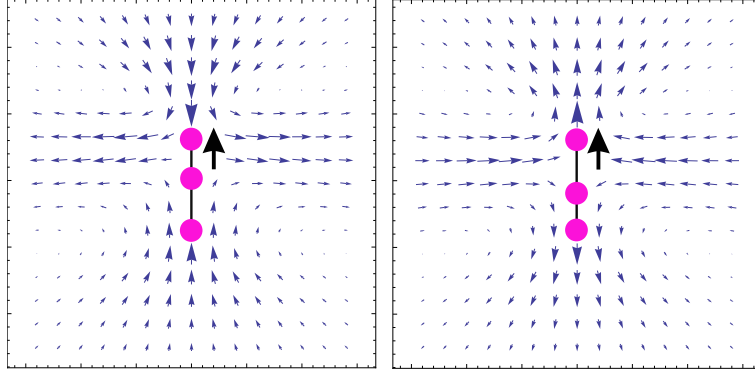


Figure 1. Velocity field of a puller (left) and a pusher (right). In both cases, the swimmer moves upward, along the bolded arrow. Velocity field decreases as $1/r^2$.

where u^f and u^b are periodic functions of time and δ is a parameter that makes the swimmer geometrically asymmetric. After solving the above equations, the average swimming velocities (linear and angular) and forces acting on the fluid read as [41]:

$$\mathbf{v}_0 = v_0 \hat{\mathbf{t}}, \quad \boldsymbol{\Omega}_0 = \mathbf{0}, \quad (4)$$

$$\langle \mathbf{f}^f \rangle = -\frac{5}{4}\pi\eta\left(\frac{a}{\ell}\right)^2\left(1 - \frac{17}{5}\delta\right)\Phi \hat{\mathbf{t}}, \quad \langle \mathbf{f}^b \rangle = -\frac{5}{4}\pi\eta\left(\frac{a}{\ell}\right)^2\left(1 + \frac{7}{5}\delta\right)\Phi \hat{\mathbf{t}}, \quad (5a)$$

where $v_0 = -\frac{7}{12}\left(\frac{a}{\ell^2}\right)(1 - \delta)\Phi$ and $\hat{\mathbf{t}}$ represents the direction of the swimmer and $\Phi = \langle u^f \dot{u}^b \rangle$ with $\langle \dots \rangle$ shows the averaging over time. Additionally $\langle \mathbf{f}^m \rangle = -\langle \mathbf{f}^b \rangle - \langle \mathbf{f}^f \rangle$. In writing the above results, we have assumed that $a \ll \ell$, $u^f \ll \ell$, $u^b \ll \ell$ and $\delta \ll 1$. Throughout this paper we choose $\Phi < 0$, so that $v_0 > 0$.

When considering the force distribution of a swimmer, the asymmetry parameter δ plays an essential role. For a symmetric swimmer ($\delta = 0$), the force distribution shows a quadrupolar field while for asymmetric case ($\delta \neq 0$) it shows a dipolar field [43]. Defining the force dipole tensor as: $\Gamma_{ij} = \sum_m x_i^m f_j^m$, we can calculate it as:

$$\boldsymbol{\Gamma} = -\frac{29}{10}f_0 \ell \delta \hat{\mathbf{t}}\hat{\mathbf{t}}, \quad (6)$$

where $f_0 = \frac{30}{7}\pi\eta a v_0$. Based on the observation that how the driving force of the motion is located at the head or at the tail of the swimmer, we can divide the dipolar swimmers to two categories of pushers and pullers. For pushers, the driving force comes from the tail while for pullers, the driving force comes from the head. In asymmetric three-sphere swimmer with $\Phi < 0$, $\delta > 0$ corresponds to a puller ($\Gamma_{tt} < 0$) and $\delta < 0$ results a pusher ($\Gamma_{tt} > 0$). For a puller (pusher), back (front) arm of the swimmer is longer than the front (back) arm. Figure 1, shows the flow field pattern for both pusher and puller. There is a fundamental difference between the flow patterns for pushers and pullers. At the next parts we will see that the hydrodynamic interaction between the swimmers will crucially depend on the sign of δ .

2.1. Long-range interactions

Since we want to consider a suspension of micro-swimmers, we need to calculate the hydrodynamic interactions between them. The above model of micro-swimmer allows us to obtain analytic formula for the interactions. The details of such calculations are similar to the case of a single swimmer and have been studied in details elsewhere [44, 45]. Here we only present the final results. Consider two swimmers located at positions \mathbf{r} and \mathbf{r}' with orientations given by $\hat{\mathbf{t}}$ and $\hat{\mathbf{t}}'$. Taking into account the hydrodynamic long-range interactions between the swimmers, the linear and angular velocities of the first swimmer averaged over the oscillations of both swimmers read as:

$$\mathbf{V}^L(\mathbf{r}, \mathbf{r}', \hat{\mathbf{t}}, \hat{\mathbf{t}}') = a_1 \left(\frac{\ell}{R}\right)^2 \mathbf{G}_1 + \left(\frac{\ell}{R}\right)^3 (a_2 \mathbf{G}_2 + a_3 \mathbf{G}_3), \quad (7)$$

$$\boldsymbol{\Omega}^L(\mathbf{r}, \mathbf{r}', \hat{\mathbf{t}}, \hat{\mathbf{t}}') = a_4 \left(\frac{\ell}{R}\right)^3 \mathbf{G}_4 + \left(\frac{\ell}{R}\right)^4 (a_5 \mathbf{G}_5 + a_6 \mathbf{G}_6). \quad (8)$$

where $\mathbf{R} = \mathbf{r} - \mathbf{r}'$ and superscript L denotes long-range interaction. The coefficients are given by:

$$\begin{aligned} a_1 &= -\frac{87}{56} \left(\frac{a}{\ell}\right) \delta v_0, & a_2 &= -\frac{6}{7} (2 + \delta) v_0, & a_3 &= -\frac{1}{2} a_2, \\ a_4 &= -\frac{1}{\ell} a_1, & a_5 &= -\frac{1}{\ell} a_2, & a_6 &= \frac{3}{2} \left(\frac{1}{\ell}\right) (2 - \delta) v_0. \end{aligned} \quad (9)$$

Regarding the above results for interaction, the terms proportional to a_1 and a_4 represent the dipolar contributions and the other terms show the quadrupolar contributions. Vectors $\mathbf{G}_1, \dots, \mathbf{G}_6$ are complex functions of relative displacement and orientation of the swimmers and are given by:

$$\mathbf{G}_1 = -3M_{ij}(\hat{\mathbf{R}}) \hat{t}'_i \hat{t}'_j \hat{\mathbf{R}}, \quad (10)$$

$$\mathbf{G}_2 = \frac{3}{2}M_{ij}(\hat{\mathbf{R}}) \hat{t}'_i \hat{t}'_j \hat{\mathbf{t}}' + \frac{3}{2}M_{ijk}(\hat{\mathbf{R}}) \hat{t}'_i \hat{t}'_j \hat{t}'_k \hat{\mathbf{R}}, \quad (11)$$

$$\mathbf{G}_3 = -3M_{ij}(\hat{\mathbf{R}}) \hat{t}'_i \hat{t}'_j \hat{\mathbf{t}} + 3M_{ijk}(\hat{\mathbf{R}}) \hat{t}'_i \hat{t}'_j \hat{t}'_k \hat{\mathbf{R}}, \quad (12)$$

$$\mathbf{G}_4 = 3M_{ijk}(\hat{\mathbf{R}}) \hat{t}'_i \hat{t}'_j \hat{t}'_k \hat{\mathbf{R}}, \quad (13)$$

$$\mathbf{G}_5 = \frac{3}{2}M_{ijk}(\hat{\mathbf{R}}) \hat{t}'_i \hat{t}'_j \hat{t}'_k \hat{\mathbf{t}}' - \frac{15}{2}M_{ijkl}(\hat{\mathbf{R}}) \hat{t}'_i \hat{t}'_j \hat{t}'_k \hat{t}'_l \hat{\mathbf{R}}, \quad (14)$$

$$\mathbf{G}_6 = -\frac{15}{2}M_{ijkl}(\hat{\mathbf{R}}) \hat{t}'_i \hat{t}'_j \hat{t}'_k \hat{t}'_l \hat{\mathbf{R}}, \quad (15)$$

where summation over repeated indices is assumed and:

$$\begin{aligned} M_{ij}(\hat{\mathbf{R}}) &= \hat{R}_i \hat{R}_j - \frac{1}{3} \delta_{ij}, & M_{ijk}(\hat{\mathbf{R}}) &= -R^4 \partial_k \left(\frac{M_{ij}}{R^3}\right), \\ M_{ijkl}(\hat{\mathbf{R}}) &= -\frac{R^5}{5} \partial_l \left(\frac{M_{ijk}}{R^4}\right), \end{aligned} \quad (16)$$

where we have used the short hand notation: $\partial_i = \partial/\partial R_i$. To obtain the above hydrodynamic interactions we have assumed that the swimmers are very far, $R \gg \ell$, and we have also averaged over the internal motion of the swimmers. As it is seen from equations (7) and (8), the first non-zero terms in the hydrodynamic interaction, the terms that are proportional to $(\ell/R)^2$ in linear velocity and $(\ell/R)^3$ in rotational velocity, are proportional to δ . This is the contribution from dipolar field of the asymmetric swimmers. Such contribution changes sign for pushers and pullers [46, 47, 48].

Rich dynamical behavior that includes coherent motion in two interacting swimmers suggests to see interesting phases in a system with many interacting swimmers [45, 49]. At next sections we will see how thermodynamic behavior of a suspension of microswimmers depends on the nature of two particle interactions.

2.2. Short-range interactions

As one can see from equations (7) and (8), the long-range hydrodynamic interactions that we have obtained are valid only at large distances, they diverge at short distances. Due to the complexity of hydrodynamics at short distances, it is not possible to obtain simple analytic results for short-range part of the interactions. We can use an approximate phenomenological model that takes into account the short-range part of the interactions. Inspired by the well known Vicsek's model [32], we consider a

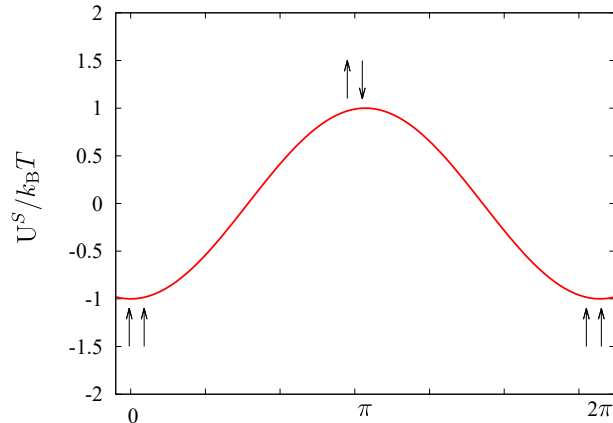


Figure 2. Short-range alignment interaction, U^S , between the swimmers is plotted as a function of the angle between their orientations. The potential has a minimum when two swimmers are aligned. Here we assumed $U_0 = 1$.

short-range interaction potential as:

$$U^S(\mathbf{r}, \mathbf{r}', \hat{\mathbf{t}}, \hat{\mathbf{t}}') = \begin{cases} -k_B T U_0 \hat{\mathbf{t}} \cdot \hat{\mathbf{t}}' & \text{for } R \leq \ell_c, \\ 0 & \text{for } R > \ell_c. \end{cases} \quad (17)$$

where ℓ_c is a crossover length-scale that separates short- and long-range interactions. We will assume that long-range hydrodynamic interactions act only for swimmers having distance larger than ℓ_c . As seen from figure 2, the above potential tends to align nearby particles. The crossover length ℓ_c has the same order of magnitude as the linear

dimension of swimmers given by 2ℓ . It should be mentioned that the above interaction does not consider all informations of the short-range interactions in real systems, this model only takes into account the steric interaction between the nearby swimmers. In terms of the potential energy, the short-range velocities can be written as:

$$\mathbf{V}^S(\mathbf{r}, \mathbf{r}', \hat{\mathbf{t}}, \hat{\mathbf{t}}') = -\frac{1}{k_B T} \mathbf{D} \cdot \nabla U^S, \quad (18)$$

$$\boldsymbol{\Omega}^S(\mathbf{r}, \mathbf{r}', \hat{\mathbf{t}}, \hat{\mathbf{t}}') = -\frac{D_R}{k_B T} \nabla_R U^S, \quad (19)$$

where ∇ and $\nabla_R \equiv \hat{\mathbf{t}} \times \partial / \partial \hat{\mathbf{t}}$ are translational and rotational gradient operators.

In above equations, \mathbf{D} is the translational diffusion tensor of a micro-swimmer and for a swimmer with elongated geometry we can decompose it to its parallel, D_{\parallel} , and perpendicular, D_{\perp} , components:

$$D_{ij} = D_{\parallel} \hat{t}_i \hat{t}_j + D_{\perp} (\delta_{ij} - \hat{t}_i \hat{t}_j), \quad (20)$$

and D_R is the rotational diffusion coefficient. Through hydrodynamic calculations, we can calculate the translational and rotational diffusion coefficients [50, 51].

Details of such calculations are presented in Appendix A. The final results are:

$$D_{\parallel} = \frac{k_B T}{18\pi\eta a} \left[1 + \frac{5}{2} \left(1 - \frac{\delta}{2} \right) \left(\frac{a}{\ell} \right) + \mathcal{O} \left(\frac{a}{\ell} \right)^2 \right], \quad (21)$$

$$D_{\perp} = \frac{k_B T}{18\pi\eta a} \left[1 + \frac{5}{4} \left(1 - \frac{\delta}{2} \right) \left(\frac{a}{\ell} \right) + \mathcal{O} \left(\frac{a}{\ell} \right)^2 \right], \quad (22)$$

$$D_R = \frac{k_B T}{12\pi\eta a \ell^2} \left[(1 - \delta) - \frac{3}{8} \left(1 - \frac{3}{2}\delta \right) \left(\frac{a}{\ell} \right) + \mathcal{O} \left(\frac{a}{\ell} \right)^2 \right], \quad (23)$$

3. Dynamics of a suspension

3.1. Langevin Dynamics

Let us consider a dilute suspension of \mathcal{N} micro-swimmers moving in a three-dimensional fluid medium with temperature T . To describe the dynamics of the suspension, we can start with Langevin description for each micro-swimmer as:

$$\partial_t \mathbf{r}_{\alpha} = v_0 \hat{\mathbf{t}}_{\alpha} + \sum_{\beta \neq \alpha} \mathbf{V}^{int}(\mathbf{r}_{\alpha}, \mathbf{r}_{\beta}, \hat{\mathbf{t}}_{\alpha}, \hat{\mathbf{t}}_{\beta}) + \boldsymbol{\eta}_{\alpha}^T(t), \quad (24)$$

$$\partial_t \hat{\mathbf{t}}_{\alpha} = \sum_{\beta \neq \alpha} \boldsymbol{\Omega}^{int}(\mathbf{r}_{\alpha}, \mathbf{r}_{\beta}, \hat{\mathbf{t}}_{\alpha}, \hat{\mathbf{t}}_{\beta}) \times \hat{\mathbf{t}}_{\alpha} + \boldsymbol{\eta}_{\alpha}^R(t), \quad (25)$$

where \mathbf{r}_{α} denotes the position vector for the hydrodynamic center of α 'th swimmer ($\alpha = 1, \dots, \mathcal{N}$) and $\hat{\mathbf{t}}_{\alpha}$ for its director. Hydrodynamic center is defined in appendix. In above relation the summation is over all other swimmers ($\beta \neq \alpha$). \mathbf{V}^{int} and $\boldsymbol{\Omega}^{int}$ are interaction contributions to the translational and rotational velocities of swimmers. We consider two types of interactions between the swimmers: a short-range alignment

interaction and a long-range one that is due to the fluid-mediated interactions between the swimmers. So \mathbf{V}^{int} and $\mathbf{\Omega}^{int}$ contain two terms:

$$\mathbf{V}^{int}(\mathbf{r}_\alpha, \mathbf{r}_\beta, \hat{\mathbf{t}}_\alpha, \hat{\mathbf{t}}_\beta) = \mathbf{V}^L + \mathbf{V}^S, \quad (26)$$

$$\mathbf{\Omega}^{int}(\mathbf{r}_\alpha, \mathbf{r}_\beta, \hat{\mathbf{t}}_\alpha, \hat{\mathbf{t}}_\beta) = \mathbf{\Omega}^L + \mathbf{\Omega}^S, \quad (27)$$

where in the last section we have obtained the long- and short-range part of the interaction. $\boldsymbol{\eta}_\alpha^T(t)$ and $\boldsymbol{\eta}_\alpha^R(t)$ are stochastic terms due to the random forces which swimmer α receives from the molecules of the ambient fluid. The random forces obey the statistics of a Gaussian noise as:

$$\langle \eta_{\alpha,i}^T(t) \eta_{\beta,j}^T(t') \rangle = D_{ij} \delta_{\alpha\beta} \delta(t - t'), \quad (28)$$

$$\langle \eta_{\alpha,i}^R(t) \eta_{\beta,j}^R(t') \rangle = D_R \delta_{ij} \delta_{\alpha\beta} \delta(t - t'). \quad (29)$$

3.2. Statistical description

In order to have a probabilistic description for a suspension composed of \mathcal{N} particles, we denote the \mathcal{N} -body probability distribution function by: $\Psi_{\mathcal{N}}(\mathbf{r}_1, \hat{\mathbf{t}}_1, \dots, \mathbf{r}_{\mathcal{N}}, \hat{\mathbf{t}}_{\mathcal{N}}, t)$. The distribution function is the probability to find the α 'th swimmer at position \mathbf{r}_α with orientation given by $\hat{\mathbf{t}}_\alpha$ at time t . This distribution function obeys the following normalization condition:

$$\prod_{\alpha=1}^{\mathcal{N}} \int d\mathbf{r}_\alpha d\hat{\mathbf{t}}_\alpha \Psi_{\mathcal{N}} = 1, \quad (30)$$

and it satisfies the following continuity equation:

$$\partial_t \Psi_{\mathcal{N}} = - \left(\sum_{\alpha=1}^{\mathcal{N}} \frac{\partial}{\partial \mathbf{r}_\alpha} \right) \cdot \mathbf{J}_{\mathcal{N}}^T - \left(\sum_{\alpha=1}^{\mathcal{N}} \hat{\mathbf{t}}_\alpha \times \frac{\partial}{\partial \hat{\mathbf{t}}_\alpha} \right) \cdot \mathbf{J}_{\mathcal{N}}^R, \quad (31)$$

where $\mathbf{J}_{\mathcal{N}}^T$ and $\mathbf{J}_{\mathcal{N}}^R$ are translational and rotational \mathcal{N} -body fluxes. At very low volume fraction of swimmers where, the distance between the swimmers is larger than the size of swimmers, we can treat the system in the mean field level. In this case the \mathcal{N} -body distribution function can be given in terms of single particle distribution function as:

$$\Psi_{\mathcal{N}} = \psi(\mathbf{r}_1, \hat{\mathbf{t}}_1, t) \cdots \psi(\mathbf{r}_{\mathcal{N}}, \hat{\mathbf{t}}_{\mathcal{N}}, t). \quad (32)$$

Using this assumption, the single particle distribution function, $\psi(\mathbf{r}, \hat{\mathbf{t}}, t)$, obeys the following Smoluchowski equation:

$$\partial_t \psi = -\nabla \cdot \mathbf{J}^T - \nabla_R \cdot \mathbf{J}^R, \quad (33)$$

where \mathbf{J}^T and \mathbf{J}^R are translational and rotational one-body fluxes and are given by:

$$\mathbf{J}^T = \left[v_0 \hat{\mathbf{t}} + \overline{\mathbf{V}}^{int} \right] \psi - \mathbf{D} \cdot \nabla \psi, \quad (34)$$

$$\mathbf{J}^R = \overline{\mathbf{\Omega}}^{int} \psi - D_R \nabla_R \psi. \quad (35)$$

Mean field translational and rotational velocities are denoted by $\overline{\mathbf{V}}^{int}$ and $\overline{\mathbf{\Omega}}^{int}$. These mean field terms should be calculated by integrating over the positions and orientations of all swimmers as:

$$\overline{\mathbf{V}}^{int}(\mathbf{r}, \hat{\mathbf{t}}, t) = \int d\mathbf{r}' d\hat{\mathbf{t}}' \mathbf{V}^{int}(\mathbf{r}, \mathbf{r}', \hat{\mathbf{t}}, \hat{\mathbf{t}}') \psi(\mathbf{r}', \hat{\mathbf{t}}', t), \quad (36)$$

$$\overline{\mathbf{\Omega}}^{int}(\mathbf{r}, \hat{\mathbf{t}}, t) = \int d\mathbf{r}' d\hat{\mathbf{t}}' \mathbf{\Omega}^{int}(\mathbf{r}, \mathbf{r}', \hat{\mathbf{t}}, \hat{\mathbf{t}}') \psi(\mathbf{r}', \hat{\mathbf{t}}', t). \quad (37)$$

In order to study the dynamics of an active system composed of interacting particles, we proceed and consider the dynamics of moments of distribution function. Density field $\rho(\mathbf{r}, t)$, polarization $\mathbf{P}(\mathbf{r}, t)$ and nematic order parameter $\mathbf{N}(\mathbf{r}, t)$ are the first three moments of the distribution function that are defined as:

$$\rho(\mathbf{r}, t) = \int d\hat{\mathbf{t}} \psi(\mathbf{r}, \hat{\mathbf{t}}, t), \quad (38)$$

$$\rho(\mathbf{r}, t) \mathbf{P}(\mathbf{r}, t) = \int d\hat{\mathbf{t}} \hat{\mathbf{t}} \psi(\mathbf{r}, \hat{\mathbf{t}}, t), \quad (39)$$

$$\rho(\mathbf{r}, t) \mathbf{N}(\mathbf{r}, t) = \int d\hat{\mathbf{t}} \left(\hat{\mathbf{t}} \hat{\mathbf{t}} - \frac{\mathbf{I}}{3} \right) \psi(\mathbf{r}, \hat{\mathbf{t}}, t). \quad (40)$$

Using equation (33), we can obtain equations that govern the dynamics of above continuum fields. As a result of such equations we see that the dynamics of n 'th moment is coupled to the dynamics of $(n - 1)$ 'th moment. So we need to cut the hierarchy at some point. As an approximation, we neglect the third (and higher) moment and cut the equations at second moment. In this case and in terms of density, polarization and nematic order, the distribution function can be constructed as:

$$\psi(\mathbf{r}, \hat{\mathbf{t}}, t) = \rho(\mathbf{r}, t) \left(\frac{1}{4\pi} + \frac{3}{4\pi} \hat{\mathbf{t}} \cdot \mathbf{P}(\mathbf{r}, t) + \frac{15}{8\pi} \left(\hat{\mathbf{t}} \hat{\mathbf{t}} - \frac{\mathbf{I}}{3} \right) : \mathbf{N}(\mathbf{r}, t) \right). \quad (41)$$

3.3. Mean field interactions

Before deriving the dynamical equations for continuum fields, we need to calculate the mean field form of interaction terms. As discussed before, the interaction between swimmers has two contributions, short- and long-range parts as:

$$\begin{aligned} \overline{\mathbf{V}}^{int}(\mathbf{r}, \hat{\mathbf{t}}, t) &= \overline{\mathbf{V}}^S + \overline{\mathbf{V}}^L \\ \overline{\mathbf{\Omega}}^{int}(\mathbf{r}, \hat{\mathbf{t}}, t) &= \overline{\mathbf{\Omega}}^S + \overline{\mathbf{\Omega}}^L. \end{aligned} \quad (42)$$

To obtain the short-range contribution we need to insert the two-body interactions from equations (18) and (19) into equations (36) and (37) then, calculate the integrations. To obtain the final results, the following integral should be performed:

$$\overline{\mathbf{U}}^S(\mathbf{r}, \hat{\mathbf{t}}, t) = \int d\mathbf{r}' d\hat{\mathbf{t}}' \mathbf{U}^S \psi(\mathbf{r}', \hat{\mathbf{t}}', t). \quad (43)$$

Now, as the interaction is short-range, we can expand $\psi(\mathbf{r}', \hat{\mathbf{t}}', t)$ as:

$$\psi(\mathbf{r}', \hat{\mathbf{t}}', t) = \psi(\mathbf{r}, \hat{\mathbf{t}}', t) + (\mathbf{r}' - \mathbf{r}) \cdot \partial_{\mathbf{r}} \psi(\mathbf{r}, \hat{\mathbf{t}}', t) + \dots, \quad (44)$$

the leading order terms will read as:

$$\bar{U}^S(\mathbf{r}, \hat{\mathbf{t}}, t) = -\frac{4}{3}\pi\ell_c^3 U_0 k_B T \left(1 + \frac{1}{10}\ell_c^2 \nabla^2 + \dots \right) (\rho \hat{\mathbf{t}} \cdot \mathbf{P}). \quad (45)$$

Now the short-range contributions will read as:

$$\begin{aligned} \bar{V}^S(\mathbf{r}, \hat{\mathbf{t}}, t) &= \frac{4}{3}\pi\ell_c^3 U_0 \mathbf{D} \cdot \nabla (\rho \hat{\mathbf{t}} \cdot \mathbf{P}) + \dots, \\ \bar{\Omega}^S(\mathbf{r}, \hat{\mathbf{t}}, t) &= \frac{4}{3}\pi\ell_c^3 U_0 D_R \nabla_R (\rho \hat{\mathbf{t}} \cdot \mathbf{P}) + \dots. \end{aligned} \quad (46)$$

Long-range contributions can also be obtained by inserting (7) and (8) into equations (36) and (37). In terms of their components, the mean field long-range interactions can be written as:

$$\bar{V}_i^L(\mathbf{r}, \hat{\mathbf{t}}, t) = b_1 T_i^1(\mathbf{r}, t) + b_2 T_i^2(\mathbf{r}, t) + b_3 T_{il}^3(\mathbf{r}, t) \hat{t}_l, \quad (47)$$

$$\bar{\Omega}_i^L(\mathbf{r}, \hat{\mathbf{t}}, t) = b_1 T_{il}^4(\mathbf{r}, t) \hat{t}_l - b_2 T_{il}^5(\mathbf{r}, t) \hat{t}_l + b_4 T_{ilm}^6(\mathbf{r}, t) \hat{t}_l \hat{t}_m, \quad (48)$$

where summation over repeated indices is assumed and the coefficients are given by:

$$\begin{aligned} b_1 &= \frac{261}{56} a \ell v_0 \delta, & b_2 &= -\frac{18}{35} \ell^3 v_0 (2 + \delta), & b_3 &= \frac{5}{2} b_2, \\ b_4 &= -\frac{45}{4} \ell^3 v_0 (2 - \delta). \end{aligned} \quad (49)$$

Functions $\mathbf{T}^1, \dots, \mathbf{T}^6$ appeared in (47) and (48) are functions of position and their detailed structures are given by:

$$T_i^1(\mathbf{r}, t) = \int d\mathbf{r}' \frac{\hat{R}_i}{R^2} M_{jk}(\hat{\mathbf{R}}) \rho(\mathbf{r}', t) N_{jk}(\mathbf{r}', t), \quad (50)$$

$$T_i^2(\mathbf{r}, t) = \int d\mathbf{r}' \frac{1}{R^3} M_{ij}(\hat{\mathbf{R}}) \rho(\mathbf{r}', t) P_j(\mathbf{r}', t), \quad (51)$$

$$T_{il}^3(\mathbf{r}, t) = \int d\mathbf{r}' \partial_l \left(\frac{M_{jk}(\hat{\mathbf{R}})}{R^3} R_i \right) \rho(\mathbf{r}', t) N_{jk}(\mathbf{r}', t), \quad (52)$$

$$T_{il}^4(\mathbf{r}, t) = \int d\mathbf{r}' \frac{\hat{R}_i}{R^3} M_{jkl}(\hat{\mathbf{R}}) \rho(\mathbf{r}', t) N_{jk}(\mathbf{r}', t), \quad (53)$$

$$T_{il}^5(\mathbf{r}, t) = \int d\mathbf{r}' \frac{1}{R^4} M_{ijl}(\hat{\mathbf{R}}) \rho(\mathbf{r}', t) P_j(\mathbf{r}', t), \quad (54)$$

$$T_{ilm}^6(\mathbf{r}, t) = \int d\mathbf{r}' \frac{\hat{R}_i}{R^4} M_{jklm}(\hat{\mathbf{R}}) \rho(\mathbf{r}', t) N_{jk}(\mathbf{r}', t). \quad (55)$$

In next sections, we will use the above results and study the dynamics of a suspension in the continuum limit.

4. Continuum description

Now we can calculate the dynamical equations for the hydrodynamic continuum fields. Starting from equation (33), multiplying both sides by powers of $\hat{\mathbf{t}}$ and integrating over solid angle spanned by $\hat{\mathbf{t}}$, we can obtain the equations that govern the dynamics of density, polarization and nematic order parameter. Results of such calculations can be written as:

$$\partial_t \rho = -v_0 \nabla \cdot (\rho \mathbf{P}) + D_1 \nabla^2 \rho + D_2 \partial_i \partial_j (\rho N_{ij}) + \dot{\rho}^L + \dot{\rho}^S, \quad (56)$$

$$\begin{aligned} \partial_t (\rho P_i) = & -v_0 \partial_j (\rho N_{ij}) - \frac{1}{3} v_0 \partial_i \rho - 2D_R \rho P_i \\ & + \partial_j \left(\frac{2}{5} D_2 \partial_i (\rho P_j) + D_3 \partial_j (\rho P_i) \right) + \dot{P}_i^L + \dot{P}_i^S, \end{aligned} \quad (57)$$

$$\begin{aligned} \partial_t (\rho N_{ij}) = & -\frac{1}{5} v_0 [\partial_i (\rho P_j) + \partial_j (\rho P_i)] + \frac{2}{15} v_0 \delta_{ij} \nabla \cdot (\rho \mathbf{P}) \\ & - 6D_R \rho N_{ij} + \frac{2}{15} D_2 \left(\partial_i \partial_j - \frac{1}{3} \delta_{ij} \nabla^2 \right) \rho \\ & + \frac{2}{7} D_2 \partial_k \left(\partial_i (\rho N_{jk}) + \partial_j (\rho N_{ik}) - \frac{2}{3} \delta_{ij} \partial_l (\rho N_{kl}) \right) \\ & + D_4 \nabla^2 (\rho N_{ij}) + \dot{N}_{ij}^L + \dot{N}_{ij}^S. \end{aligned} \quad (58)$$

As one can see, in addition to the diffusion and swimmer's activity terms, the terms proportional to v_0 , there are contributions from interactions. Contributions from long-range and short-range interactions are collected in terms that are denoted by superscripts L and S respectively ($\dot{\rho}^L$, $\dot{\rho}^S$ and *etc.*). To keep the continuity of text, we put these interaction terms in Appendix B. Effective diffusion coefficients appeared in the above equations are defined as:

$$\begin{aligned} D_1 &= \frac{1}{3} (D_{\parallel} + 2D_{\perp}), & D_2 &= D_{\parallel} - D_{\perp}, \\ D_3 &= \frac{1}{5} (D_{\parallel} + 4D_{\perp}), & D_4 &= \frac{1}{7} (D_{\parallel} + 6D_{\perp}). \end{aligned} \quad (59)$$

4.1. Steady state solutions

Here we seek for steady state uniform solutions of the above dynamical equations for continuum fields. Terms corresponding to long-range interactions and swimmer's activity, do not contribute in the uniform steady state solutions. Steady states are solutions to the following equations:

$$\partial_t \rho = 0, \quad (60)$$

$$\partial_t (\rho P_i) = -2D_R \rho P_i + \frac{4}{3} \pi D_R \ell_c^3 U_0 \rho^2 \left(\frac{2}{3} P_i - P_j N_{ij} \right), \quad (61)$$

$$\partial_t (\rho N_{ij}) = -6D_R \rho N_{ij} + \frac{8}{5} \pi D_R \ell_c^3 U_0 \rho^2 \left(P_i P_j - \frac{P^2}{3} \delta_{ij} \right). \quad (62)$$

As a result of the above equations, we realize that there are two different homogenous steady state phases in our system. The first phase, denoted by phase I , is an isotropic phase and defined by:

$$\rho^I = \rho_0, \quad \mathbf{P}^I = \mathbf{0}, \quad \mathbf{N}^I = \mathbf{0}. \quad (63)$$

In this phase, all swimmers are distributed uniformly in the fluid and move randomly without any preferred direction. Increasing the density, we see that beyond a critical density $\rho_0 > \rho_c = 9/(4\pi\ell_c^3 U_0)$, a homogeneous polarized state appears. This phase is denoted by phase P and defined by:

$$\rho^P = \rho_0, \quad \mathbf{P}^P = \mathbf{P}^\infty, \quad \mathbf{N}^P = \mathbf{N}^\infty. \quad (64)$$

In this polarized phase, swimmers are distributed uniformly and move in a preferred direction. Steady state polarization and nematic order parameter in the polar phase are given by:

$$\mathbf{P}^\infty = \sqrt{\frac{15}{4\pi\ell_c^3\rho_0 U_0} \left(1 - \frac{9}{4\pi\ell_c^3\rho_0 U_0}\right)} \hat{\mathbf{n}}, \quad (65)$$

$$\mathbf{N}^\infty = \left(1 - \frac{9}{4\pi\ell_c^3\rho_0 U_0}\right) \left(\hat{\mathbf{n}}\hat{\mathbf{n}} - \frac{\mathbf{I}}{3}\right), \quad (66)$$

where $\hat{\mathbf{n}}$ denotes the direction of broken symmetry. Figure 3, shows a phase diagram in a space characterized by U_0 and $\rho_0\ell_c^3$. Appearance of the ordered phase is a direct

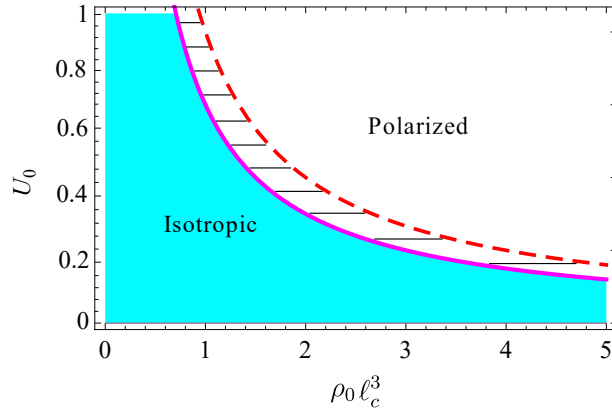


Figure 3. Phase diagram showing possible thermodynamic phases for a suspension of swimmers. Isotropic and polarized phases are separated by a solid line in a space given by U_0 (strength of short-range interaction) and $\rho_0\ell_c^3$ (density of swimmers). Taking into account long-wavelength fluctuations, calculations show that both phases are unstable. Part of polarized phase denoted by dashed lines, shows the states that are stable with respect to splay fluctuations. These states are unstable with respect to bend fluctuations.

consequence of the short-range (alignment) interaction between the swimmers. As it is apparent from the equations, long-range interactions alone, are not able to induce any ordered state in bulk [21]. It is shown very recently that short-range hydrodynamic interactions in symmetric squirmers are also able to induce a polar state [52].

4.2. Stability of Isotropic state

In addition to existence of steady state phases, their stability is important to analyze. Thermal or non-thermal fluctuations can destabilize the above steady state phases. In this section, we study the stability of the steady state solutions.

To study the stability of isotropic phase, we add small fluctuations to the corresponding fields of the isotropic state and investigate their dynamics:

$$\rho(\mathbf{r}, t) = \rho_0 + \delta\rho(\mathbf{r}, t), \quad (67)$$

$$\mathbf{P}(\mathbf{r}, t) = \mathbf{0} + \delta\mathbf{P}(\mathbf{r}, t), \quad (68)$$

$$\mathbf{N}(\mathbf{r}, t) = \mathbf{0} + \delta\mathbf{N}(\mathbf{r}, t). \quad (69)$$

Using the dynamical equations obtained in the above section, we can obtain the evolution equations of these fluctuating fields. To linearize the equations, we introduce spatial Fourier transformation as:

$$\check{f}(\mathbf{k}) = \int d\mathbf{r} e^{i\mathbf{k}\cdot\mathbf{r}} f(\mathbf{r}). \quad (70)$$

In Appendix B, we have shown how a typical term in the dynamical equation can be linearized. Repeating the same procedure for all other terms, we can arrive at the following equations that describe the linearized dynamics of the fluctuations around the isotropic phase:

$$\partial_t \delta\check{\rho} = iv_0 \rho_0 k_i \delta\check{P}_i - \frac{8\pi i}{9} b_2 \rho_0^2 k_i \delta\check{P}_i - D_1 k^2 \delta\check{\rho} - \rho_0 D_2 k_i k_j \delta\check{N}_{ij}, \quad (71)$$

$$\begin{aligned} \partial_t \delta\check{P}_i &= iv_0 k_j \delta\check{N}_{ij} + i \frac{v_0}{3\rho_0} \delta\check{\rho} k_i - \frac{8\pi i}{45} b_3 \rho_0 k_j \delta\check{N}_{ij} - \frac{2}{5} D_2 k_j \delta\check{P}_j k_i - D_3 k^2 \delta\check{P}_i \\ &+ \frac{4}{9} \pi \ell_c^3 U_0 \rho_0 \left(\frac{1}{5} D_2 [2k_j \delta\check{P}_j k_i + k^2 \delta\check{P}_i] + D_\perp k^2 \delta\check{P}_i \right) - 2D_R \delta\check{P}_i \\ &+ \frac{8}{9} \pi D_R \ell_c^3 U_0 \rho_0 \delta\check{P}_i - \frac{32\pi i}{225} b_4 \rho_0 k \left(-\hat{k}_j \hat{k}_k \delta\check{N}_{jk} \hat{k}_i + \frac{14}{35} \delta\check{N}_{ik} \hat{k}_k \right) \end{aligned} \quad (72)$$

and

$$\begin{aligned} \partial_t \delta\check{N}_{ij} &= \frac{2}{5} iv_0 \left(\frac{1}{2} [k_i \delta\check{P}_j + k_j \delta\check{P}_i] - \frac{1}{3} k_k \delta\check{P}_k \delta_{ij} \right) - \frac{2}{15\rho_0} D_2 k_i k_j \delta\check{\rho} \\ &+ \frac{2}{45} D_2 k^2 \delta_{ij} \frac{\delta\check{\rho}}{\rho_0} - 6D_R \delta\check{N}_{ij} - D_4 k^2 \delta\check{N}_{ij} - \frac{2}{7} D_2 \left(k_z k_i \delta\check{N}_{jz} \right. \\ &+ k_z k_j \delta\check{N}_{iz} - \frac{2}{3} \delta_{ij} k_k k_l \delta\check{N}_{kl} \left. \right) + \frac{\rho_0}{5} \left(\frac{8\pi}{3} b_1 [2\hat{k}_k \hat{k}_l \delta\check{N}_{kl} \hat{k}_i \hat{k}_j \right. \\ &- \delta\check{N}_{ik} \hat{k}_k \hat{k}_j - \delta\check{N}_{jk} \hat{k}_k \hat{k}_i + \frac{2}{5} \delta\check{N}_{ij}] + \frac{8\pi i}{15} b_2 [5k_k \delta\check{P}_k \hat{k}_i \hat{k}_j \\ &\left. - \delta\check{P}_i k_j - \delta\check{P}_j k_i - k_k \delta\check{P}_k \delta_{ij}] \right). \end{aligned} \quad (73)$$

These coupled equations, govern the dynamics of fluctuations. As the analysis of above coupled equations is not simple, we can use different approximations to understand physical mechanisms of possible instabilities.

As a first approximation and at times longer than time scale of rotational diffusion ($t \gg D_R^{-1}$), we can neglect the dynamics of $\delta\check{P}_i$ and $\delta\check{N}_{ij}$ in equations (72) and (73). Solving the simplified equations for polarization and nematic fluctuations ($\partial_t\delta\check{P}_i = \partial_t\delta\check{N}_{ij} \rightarrow 0$), we can substitute them in equation (71) and keep leading order powers of wave vector k . This will result an effective diffusion equation for density fluctuations as:

$$\partial_t\delta\check{\rho} = -D_{eff}k^2\delta\check{\rho}, \quad (74)$$

where the effective diffusion constant is given by:

$$D_{eff} = D_1 + \frac{v_0^2}{D_R(3 - \frac{4}{3}\pi\ell_c^3\rho_0U_0)} \left[\frac{1}{2} + \frac{8\pi\rho_0\ell^3}{35} \right]. \quad (75)$$

Since in the isotropic phase $\ell_c^3\rho_0U_0 < 9/4\pi$, the above effective diffusion coefficient is always positive and it is greater than diffusion coefficient of a brownian self-propelled rod, $D_1 + v_0^2/6D_R$ [53]. As a result of positivity of D_{eff} , density fluctuations damp and the isotropic state is stable if we neglect polarization and nematic fluctuations.

It is a well known fact that for an active brownian particle, orientational fluctuations increase the translational diffusion by a term proportional to v_0^2/D_R , but what is new here is the effect of hydrodynamic interactions. In the above result, the second term in bracket, $(8\pi/35)\rho_0\ell^3$, which is due to hydrodynamic interaction, shows that the hydrodynamic interaction speeds up the diffusion process. The increase in diffusion due to the hydrodynamic interaction is proportional to the density of swimmers and also the size of an individual swimmer.

To have more insights on the fluctuations in the isotropic phase, we study the dispersion relation for hydrodynamic modes in the system. In this case, we do not base our approximation on neglecting the dynamics of polarization and nematic order parameter from above coupled equations. It is apparent from equations (72) and (73) that the nematic fluctuations are coupled to density fluctuations in higher powers of wave vector. We are interested in the long-wavelength fluctuations so, as an another approximation we may discard nematic fluctuations ($\delta\check{N}_{ij} \rightarrow 0$) and consider only the coupled dynamics of density and polarization fluctuations. Assuming a time dependent form for the fluctuations as:

$$\delta\check{\rho}, \delta\check{P}_i \sim e^{\chi(k)t}, \quad (76)$$

we can study their coupled dynamics and obtain a dispersion relation like $\chi = \chi(k)$. Up to the leading orders of k , dispersion relations read:

$$\begin{aligned} \chi_{\pm} = & \frac{1}{54} \left[-9 \left(3 - \frac{4}{3}\pi\ell_c^3\rho_0U_0 \right) (2D_R + D_5k^2) - 27D_1k^2 \right. \\ & \pm \left[\left(9 \left(3 - \frac{4}{3}\pi\ell_c^3\rho_0U_0 \right) (2D_R + D_5k^2) + 27D_1k^2 \right)^2 \right. \\ & \quad \left. + 108 \left(-9D_1k^2 \left(3 - \frac{4}{3}\pi\ell_c^3\rho_0U_0 \right) (2D_R + D_5k^2) \right. \right. \\ & \quad \left. \left. - 9v_0^2k^2 \left(1 + \frac{16\pi}{35}\rho_0\ell^3(2 + \delta) \right) \right) \right]^{1/2} \Big], \quad (77) \end{aligned}$$

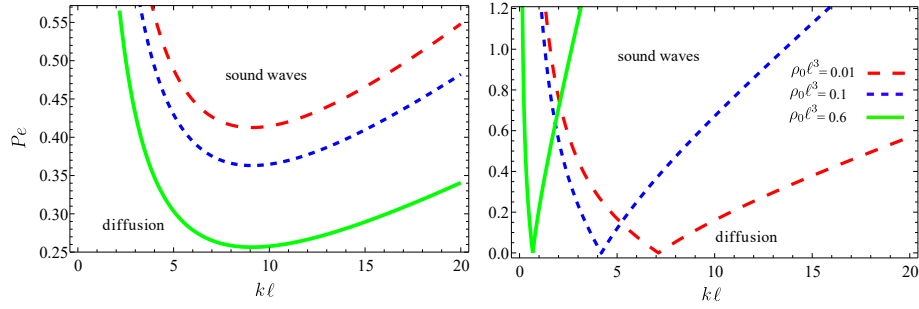


Figure 4. For a system with given $\rho_0 \ell^3$ and depending on the value of Péclet number $Pe = \frac{v_0 \ell}{D_{\parallel}}$, a fluctuating mode with wave vector $k\ell$, can propagate with diffusion or sound wave mechanism. Lines show the boundary between these two different behavior. Left graph is for a system that has only long-range interactions but the right graph shows the results for a system that has both short- and long-range interactions. Numerical values we have used are: $\delta = 0.1$, $a/\ell = 0.1$, $\ell_c/\ell = 1$ and $U_0 = 1$.

where $D_5 = 1/5(3D_{\parallel} + 2D_{\perp})$. As we expected from previous discussion, for $\ell_c^3 \rho_0 U_0 < 9/4\pi$, both χ_+ and χ_- are negative, reflecting the fact that the isotropic phase is always stable. It should be also noted that albeit the two modes have always negative real values, but if the self-propulsion speed of the swimmers is greater than a threshold value, they will have an imaginary part. As a result of this imaginary part, fluctuations of density and polarization will decay with a propagating mechanism and propagating sound waves will appear in the system [54]. In terms of Péclet number $Pe = (v_0 \ell)/D_{\parallel}$ and dimensionless wave vector $k\ell$, figure 4, shows the regions where these waves can propagate. For an intermediate $k\ell$, density waves appear at larger Pe . As seen in figure 4 (left), taking into account only long-range part of the interactions, increasing the density will decrease the threshold Pe above which propagating waves appear. Taking into account both long- and short-range interactions in figure 4 (right), we see that smaller densities of swimmers have a wider region for density waves. Interestingly, all these results are valid for both pushers and pullers.

Above approximations show that density and polarization fluctuations are not able to induce any instability in the isotropic phase. To see how the nematic fluctuations can provide mechanism for instability, we can study its dynamics separately. Arranging the right hand side of equation (73) in powers of k , we can study the nematic fluctuations at long-wavelength limit. Keeping the leading order term, we find that the nematic fluctuations are decoupled from density and polarization as:

$$\partial_t \delta N_s = \left(-6D_R + \frac{16\pi}{75} \rho_0 b_1 \right) \delta N_s, \quad (78)$$

$$\partial_t \delta \mathbf{N}_b = \left(-6D_R - \frac{8\pi}{25} \rho_0 b_1 \right) \delta \mathbf{N}_b, \quad (79)$$

where nematic fluctuations are decomposed into their splay, $\delta N_s = \hat{\mathbf{k}} \cdot \delta \check{\mathbf{N}} \cdot \hat{\mathbf{k}}$, and bend $\delta \mathbf{N}_b = \hat{\mathbf{k}} \cdot \delta \check{\mathbf{N}} \cdot (\mathbf{I} - \hat{\mathbf{k}}\hat{\mathbf{k}})$ components. Coefficient b_1 is proportional to the

asymmetry parameter δ and for pullers (pushers) it is positive (negative). This shows that, if the density of swimmers is greater than a value given by $\rho_{ins} \propto D_R/|b_1|$, splay (bend) perturbations in nematic tensor can destabilize an isotropic suspension of pullers (pushers). Such resolution in the instability of pushers and pullers will be seen at the next section.

4.3. Stability of Polar state

To study the stability of polar phase, we assume that the density of swimmers is larger than ρ_c , so that the polarized phase has been established. Then we study the dynamics of fluctuations around the polarized state. Denoting by $\hat{\mathbf{n}}$, the direction of polarization, we suppose that the order parameter has a constant value but its direction fluctuates. In this case, hydrodynamic fields can be written as:

$$\rho = \rho_0 + \delta\rho, \quad (80)$$

$$\mathbf{P} = P^\infty (\hat{\mathbf{n}}_0 + \delta\mathbf{n}), \quad (81)$$

$$\mathbf{N} = N^\infty \left((\hat{\mathbf{n}}_0 + \delta\mathbf{n})(\hat{\mathbf{n}}_0 + \delta\mathbf{n}) - \frac{\mathbf{I}}{3} \right). \quad (82)$$

Where we have assumed $\hat{\mathbf{n}} = \hat{\mathbf{n}}_0 + \delta\mathbf{n}$, with $\hat{\mathbf{n}}_0$ is the average direction of polarization in system. Furthermore for small fluctuations we have $\hat{\mathbf{n}}_0 \cdot \delta\mathbf{n} = 0$. Using the above definitions, we can linearize equations (56) and (57) and obtain evolution equations for density and director fluctuations. Since we are doing our calculations in the Fourier space, the angle between wave vector \mathbf{k} and director $\hat{\mathbf{n}}_0$ will emerge in the linearized equations. To simplify the analysis, we decompose the fluctuations into bend and splay distortions. Splay distortion is a fluctuation with $\nabla \cdot \mathbf{P} \neq 0$ ($\nabla \cdot \delta\mathbf{n} \neq 0$) and for bend fluctuations $\mathbf{P} \times (\nabla \times \mathbf{P}) \neq 0$ ($\nabla \times \delta\mathbf{n} \neq 0$). Decomposing the wave vector \mathbf{k} into its parallel and perpendicular components as: $\mathbf{k} = (\mathbf{k} \cdot \hat{\mathbf{n}}_0)\hat{\mathbf{n}}_0 + \mathbf{k}_\perp$, we can see that for bend (splay) fluctuations only the parallel (perpendicular) component of the wave vector contributes. These two modes of fluctuations are independent and this allows us to study them separately.

To study the bend fluctuations, we can set $\mathbf{k} = k\hat{\mathbf{n}}_0$ and study the dynamics of fluctuations. Using a linearization procedure similar to what we have used at previous section and keeping terms up to second order of wave vector, we can arrive at the following equations for bend fluctuations:

$$\partial_t \delta\check{\rho}_b = (i\chi_\rho^{Im} + \chi_\rho^{Re}) \delta\check{\rho}_b, \quad (83)$$

$$\partial_t \delta\check{\mathbf{n}}_b = (i\chi_n^{Im} + \chi_n^{Re}) \delta\check{\mathbf{n}}_b, \quad (84)$$

where the imaginary and real parts are given by:

$$\chi_\rho^{Re} = -\frac{16\pi}{9}\rho_0 N^\infty b_1 + k^2 (-D_1 + N^\infty D_6), \quad (85)$$

$$\chi_\rho^{Im} = P^\infty k \left(v_0 - \frac{8\pi}{9}\rho_0 b_2 + \frac{64\pi}{45}\rho_0 N^\infty b_3 \right), \quad (86)$$

$$\chi_n^{Re} = -\frac{136\pi}{75}b_1\rho_0N^\infty + \frac{4}{35}k^2 D_2 \left(\frac{4}{3}\pi\ell_c^3\rho_0U_0 - 3 \right), \quad (87)$$

$$\chi_n^{Im} = \frac{k}{\rho_0 P^\infty} \left(v_0\rho_0N^\infty - \frac{8\pi}{45}\rho_0^2b_3N^\infty(1 - N^\infty) - \frac{4\pi}{25}b_2\rho_0^2P^{\infty 2} - b_4\rho_0^2N^\infty \left[\frac{2368}{(105)^2}N^\infty + \frac{192}{875} \right] \right), \quad (88)$$

with $D_6 = 1/3(7D_{\parallel} + 8D_{\perp})$. As it is seen from the above equations, fluctuations of density and polarization are decoupled for the case of bend distortions. Both of modes show that sound-like density waves can propagate in the system; regions with dense ordered population of particles propagating in a disordered background. Propagation of these waves is a signature of Vicsek-type flocking models [33, 17].

To analyze the stability of polar state against bend fluctuations, let us consider two cases, first: without hydrodynamic interactions and second: with hydrodynamic interactions. The terms proportional to b_i in the above equations, originate from long-range hydrodynamic interactions. In the absence of hydrodynamic interactions where $b_i = 0$, real parts in both of the above equations are of order k^2 , revealing the diffusing nature of the fluctuations. Moreover, under these conditions density fluctuations are damped for $\ell_c^3\rho_0U_0 < \frac{3}{4\pi} \frac{7D_{\parallel} + 8D_{\perp}}{2(D_{\parallel} + D_{\perp})} \sim 0.9$ (we used numerical values as: $\delta = 0.1$ and $a/\ell = 0.1$). These states are denoted by dashed region in figure 3. Beyond this region and for $\ell_c^3\rho_0U_0 > 0.9$, density fluctuations can grow and form clusters of swimmers. Considering the polarization fluctuations, we can see that for $\ell_c^3\rho_0U_0 > 9/4\pi$, such fluctuations can always grow and make the polar state unstable.

Taking into account both short- and long-range interactions and in the limit of long-wavelength fluctuations ($k \rightarrow 0$), the terms that are proportional to b_1 in (85) and (87), are the most important terms that determine the instability criterion. Recalling the fact that $b_1 \propto \delta$, we see that for pullers ($\delta > 0$) density and director fluctuations diminish, but they diverge for pushers ($\delta < 0$). The growth of bend fluctuations destabilizes any polar order in a suspension of pushers [36].

To study the role of splay fluctuations, we set $\mathbf{k} = \mathbf{k}_{\perp} = k\hat{\mathbf{n}}_{\perp}$, with $\hat{\mathbf{n}}_{\perp} \cdot \hat{\mathbf{n}}_0 = 0$. For splay distortions, fluctuations of density and director are always coupled to each other and they obey the following equations:

$$\partial_t \delta \check{\rho}_s = H_{11} \delta \check{\rho}_s + H_{12} \delta \check{n}_s, \quad (89)$$

$$\partial_t \delta \check{n}_s = H_{21} \delta \check{\rho}_s + H_{22} \delta \check{n}_s, \quad (90)$$

where

$$H_{11} = \frac{8}{9}\pi b_1 \rho_0 N^\infty + k^2 (-D_1 + N^\infty D_7), \quad (91)$$

$$H_{12} = ik\rho_0 P^\infty \left(v_0 i - \frac{8}{9}\pi b_2 \rho_0 - \frac{2}{5}\pi b_3 \rho_0 N^\infty \right), \quad (92)$$

$$H_{21} = \frac{ik}{\rho_0 P^\infty} \left(\frac{1}{3} v_0 (1 - N^\infty) + \frac{32\pi}{135} \rho_0 b_3 N^\infty \left(\frac{2}{7} N^\infty - 1 \right) - \frac{4\pi}{25} \rho_0 b_2 P^{\infty 2} - \frac{16\pi}{175} \rho_0 b_4 N^\infty \left(\frac{6}{5} + \frac{29}{63} N^\infty \right) \right), \quad (93)$$

$$H_{22} = \frac{64\pi}{75} b_1 \rho_0 N^\infty - \frac{3}{35} D_2 k^2 \left(\frac{4}{3} \pi \ell_c^3 \rho_0 U_0 - 3 \right), \quad (94)$$

with $D_7 = 1/3(4D_{\parallel} + 11D_{\perp})$ and $\delta \tilde{n}_s = \hat{\mathbf{n}}_{\perp} \cdot \delta \tilde{\mathbf{n}}$. By calculating eigenvalues of matrix \mathbf{H} , we will obtain two dispersion relations for the fluctuation spectrum. In the absence of hydrodynamic interactions, the spectrum of fluctuation has a simpler form:

$$\chi_{\pm} = \pm \frac{ikv_0}{\sqrt{\frac{4}{3}\pi\ell_c^3\rho_0U_0}} + k^2 \left(D_8 - \frac{3D_9}{4\pi\ell_c^3\rho_0U_0} - \frac{2}{35}\pi\ell_c^3\rho_0U_0D_2 \right), \quad (95)$$

where $D_8 = 2/35(11D_{\parallel} + 24D_{\perp})$, $D_9 = 1/2(4D_{\parallel} + 11D_{\perp})$. Real part of this relation is negative for $\ell_c^3\rho_0U_0 < 0.9$, reflecting the fact that in the absence of hydrodynamic interactions, splay fluctuations will decay to zero when $9/4\pi < \ell_c^3\rho_0U_0 < 0.9$, (dashed region in figure 3). But for $\ell_c^3\rho_0U_0 > 0.9$, above the red dashed line in figure 3, splay fluctuations diverge, hence make the polarized state unstable.

If we consider the contributions from hydrodynamic interactions and in long-wavelength limit, the dispersion relations for the splay fluctuations read as:

$$\chi_+ = \frac{4}{5}\pi\rho_0N^\infty b_1 + \mathcal{O}(k)^2, \quad \chi_- = \frac{1}{5}\pi\rho_0N^\infty b_1 + \mathcal{O}(k)^2. \quad (96)$$

As for the bend fluctuations, the sign of $b_1 \propto \delta$ determines the criterion for instability. For a suspension of pullers ($b_1 > 0$) fluctuations grow but for pushers ($b_1 < 0$) fluctuations damp to zero. So an ordered suspension of pullers becomes unstable by the growth of splay fluctuations.

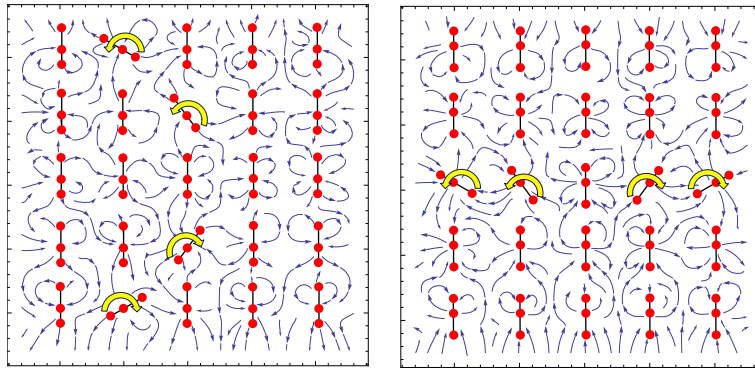


Figure 5. Flow patterns for demonstrating bend (left) and splay (right) distortions in polarized phase. An ordered suspension of pushers (pullers) is unstable due to the growth of bend (splay) fluctuations. Small arrows show the direction of flow field in the inter particle regions and large arrows show the flow field calculated at the position of distorted swimmers.

5. Summary and Discussion

In this article, we have started from a microscopic model for a hydrodynamic microswimmer and have derived its average dynamical characteristics such as velocity and force distribution. The swimmer that we have started with, is able to model both pushers and pullers. We have shown that a set of analytical expressions can be obtained for the long-range interactions between two swimmers. Extending the system to a three dimensional dilute suspension of swimmers and considering two body interaction between swimmers, we have developed a continuum description that can capture thermodynamic properties of the suspension. Furthermore, we assumed that in addition to long-range interactions, there is a short-range interaction that can align the nearby swimmers.

What we aimed in this article was to investigate the role of interactions in long-wavelength instabilities of the suspension. Isotropic phase and a symmetry broken polar phase, are two possible thermodynamic phases of the system. Depending on the density of swimmers, at low density of swimmers, the system is in isotropic phase and increasing the density will lead the system to a polar phase. In a system with hydrodynamic interactions, both of the above phases are unstable with respect to long-wavelength fluctuations. It is the long-range interaction that initiates the instability in an interacting suspension. Our results are compatible with the well known results of phenomenological models that state the origin of instability. Decomposing the nematic distortions into bend and splay fluctuations, we show that for a suspension of pushers, bend fluctuations mediate the instability and for a suspension of pullers it is the splay fluctuation that initiates the instability. Intuitional arguments can help to have more insights on the instability of polar phase. Figure 5(left), shows a regular collection of pushers with polar order. A small bend fluctuation is introduced to this collection by distorting the director of five selected swimmers. For a regular system, fluid velocity due to the other swimmers averages to zero at the position of each swimmer, but for the distorted case shown in this figure, fluid velocity has nonzero value at the position of distorted swimmers. As shown by large arrows, the velocity streamlines at the position of distorted swimmers are in the direction that tend to increase the initial distortions and destroy the initial regular state. Figure 5(right), shows the case for pullers with a small splay fluctuation. For pullers, by applying a small splay fluctuation, the system will tend to increase it and destroy the polar order.

Another interesting feature in active nematic is the appearance of bands in polar state. In symmetry broken polar phase, density waves will appear. Imaginary parts appeared in equations (86), (88) and (95), reflect this fact. Interestingly, in the case of splay fluctuations, a single group velocity for these traveling waves is seen. Finally, we should mention that all instabilities arized from hydrodynamic interactions, are for dipolar swimmers. For a collection of neutral swimmers with quadrupolar force distributions, the terms proportional to b_1 in equations (47) and (48) do not contribute and all ordered phases are stable with respect to long-wavelength fluctuations.

Acknowledgement

Useful discussions with M. C. Marchetti and K. Kruse are acknowledged.

Appendix A. Hydrodynamic center and diffusion coefficients for a rigid swimmer

Here we want to show how the hydrodynamic center and diffusion coefficients for a swimmer can be calculated. Let us consider a rigid swimmer composed of three spheres with equal radii a , linked linearly by two negligible diameter linkers. Labeling spheres by f , m and b , the front linkage has a length given by $L^f = \ell$ and the back linkage has a length given by $L^b = \ell(1 + \delta)$. Hydrodynamic center for this rigid system is a point around which the translational motion is independent from the rotational motion. As a result of symmetry, for our linear three linked spheres, the hydrodynamic center lies somewhere on the longer linkage with a distance x from the middle sphere. Hydrodynamic center is a geometrical concept and it is independent from dynamics, but we can benefit any dynamical problem to calculate it. Let us consider a dynamical problem that as a result of an external force, the hydrodynamic center moves linearly without any net rotation. With respect to hydrodynamic center, total torque should vanish: $x f_{\perp}^m + (\ell + x) f_{\perp}^f - (\ell(1 + \delta) - x) f_{\perp}^b = 0$ where, \perp denotes the components of vectors perpendicular to the linkages. In addition to this condition, there is a set of linear equations that relates the forces and velocities as: $\mathbf{v}^{\alpha} = \sum_{\beta=f,m,b} O^{\alpha\beta} \mathbf{f}^{\beta}$ where O denotes the Oseen's tensor. We can use this set of equations and find relations between perpendicular components of forces and velocities. Rigidity condition is another equation that we must consider: $v_{\perp}^f = v_{\perp}^m = v_{\perp}^b$. Using the rigidity and force-velocity equations we can obtain relations for f_{\perp}^f/f_{\perp}^m and f_{\perp}^b/f_{\perp}^m and plugging them into the torque free condition, we can obtain the following result for x :

$$x = \frac{1}{3}\delta \left(\ell + \frac{7}{8}a \right). \quad (\text{A.1})$$

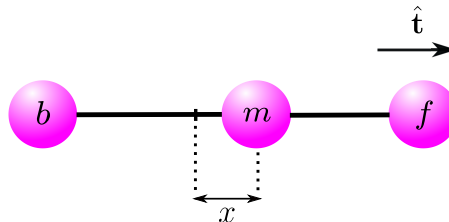


Figure A1. In an asymmetric three-sphere swimmer, hydrodynamic center is located at a distance x from the middle sphere.

Having in hand the position of hydrodynamic center, we can calculate the translational and rotational diffusion coefficients. To obtain the translational diffusion coefficients, let us apply an external force \mathbf{f}_T to the system and calculate the linear velocity \mathbf{v}_T that the system will acquire. Then the translational diffusion matrix \mathbf{D}

is defined by: $\mathbf{v}_T = (k_B T)^{-1} \mathbf{D} \cdot \mathbf{f}_T$. To calculate \mathbf{D} , one should note that in addition to force-velocity relations, constraints of total force $\mathbf{f}^f + \mathbf{f}^m + \mathbf{f}^b = \mathbf{f}_T$ and rigidity $\mathbf{v}^f = \mathbf{v}^m = \mathbf{v}^b = \mathbf{v}_T$ should be considered. Solving these equations, we will have:

$$(k_B T)^{-1} D_{ij} = K(\ell) \hat{t}_i \hat{t}_j + K(2\ell) (\delta_{ij} - \hat{t}_i \hat{t}_j), \quad (\text{A.2})$$

where

$$K(\ell) = \frac{1}{18\pi\eta a} \left[1 + \frac{5}{2} \left(1 - \frac{\delta}{2} \right) \left(\frac{a}{\ell} \right) + \mathcal{O} \left(\frac{a}{\ell} \right)^2 \right], \quad (\text{A.3})$$

In terms of its parallel and perpendicular components, the diffusion coefficients are given by: $D_{\parallel} = k_B T K(\ell)$ and $D_{\perp} = k_B T K(2\ell)$.

To calculate the rotational diffusion coefficient, we apply an external torque τ around the hydrodynamic center, then the system will rotate with angular velocity Ω around that center with no translation for hydrodynamic center. Rotational diffusion can be calculated as: $\Omega = (k_B T)^{-1} D_R \tau$. In this case, in addition to the linear force-velocity relations given by Oseen's tensor, we must consider the torque equation as $\tau = x f_{\perp}^m + (\ell + x) f_{\perp}^f - (\ell(1 + \delta) - x) f_{\perp}^b$ and rigidity constraints as: $v_{\perp}^m = x\Omega$, $v_{\perp}^f = (\ell + x)\Omega$ and $v_{\perp}^b = -(\ell(1 + \delta) - x)\Omega$. Solving all these equations simultaneously, the final result reads as:

$$D_R = \frac{k_B T}{12\pi\eta a \ell^2} \left[(1 - \delta) - \frac{3}{8} \left(1 - \frac{3}{2}\delta \right) \left(\frac{a}{\ell} \right) + \mathcal{O} \left(\frac{a}{\ell} \right)^2 \right]. \quad (\text{A.4})$$

Appendix B. Details of interaction terms

In this appendix we give the details of interaction contributions introduced in equations (56), (57) and (58). Interaction contributions to the dynamics of density, polarization and nematic order parameter read as:

$$\dot{\rho}^L = -\partial_i \left([b_1 T_i^1 + b_2 T_i^2] \rho + b_3 T_{il}^3 \rho P_l \right). \quad (\text{B.1})$$

$$\begin{aligned} \dot{\rho}^S = -\frac{4}{3} \pi \ell_c^3 U_0 \partial_i \left(\rho \partial_j (\rho P_k) \left(\frac{1}{5} D_2 (\delta_{kj} P_i + \delta_{ik} P_j + \delta_{ij} P_k) \right. \right. \\ \left. \left. + D_{\perp} \delta_{ij} P_k \right) \right). \end{aligned} \quad (\text{B.2})$$

$$\begin{aligned} \dot{P}_i^L = -\partial_j \left((b_1 T_j^1 + b_2 T_j^2) \rho P_i + b_3 T_{jl}^3 \rho \left(N_{il} + \frac{\delta_{il}}{3} \right) \right) \\ + \frac{4}{5} (b_1 T_{il}^4 - b_2 T_{il}^5) \rho P_l - \frac{1}{5} b_1 T_{ll}^4 \rho P_i + \frac{6}{7} b_4 T_{ilm}^6 \rho N_{lm} \\ - \frac{1}{5} (b_1 T_{li}^4 - b_2 T_{li}^5) \rho P_l - \frac{2}{7} b_4 T_{mlm}^6 \rho N_{li} - \frac{18}{35} b_4 T_{lli}^6 \rho \\ - \frac{2}{7} b_4 T_{lim}^6 \rho N_{lm}. \end{aligned} \quad (\text{B.3})$$

$$\begin{aligned}
\dot{P}_i^S = & -\frac{4}{3}\pi\ell_c^3 U_0 \partial_j \left(D_2 \frac{\rho}{7} \left(\frac{7}{15} [\partial_i(\rho P_j) + \partial_j(\rho P_i) + \delta_{ij} \nabla \cdot (\rho \mathbf{P})] \right. \right. \\
& + \partial_k(\rho P_j) N_{ik} + \partial_j(\rho P_l) N_{li} + \partial_k(\rho P_i) N_{kj} + \nabla \cdot (\rho \mathbf{P}) N_{ij} \\
& \left. \left. + \partial_k(\rho P_l) N_{lk} \delta_{ij} + \partial_i(\rho P_l) N_{lj} \right) + D_{\perp} \rho \left(\partial_j(\rho P_l) N_{li} + \frac{1}{3} \partial_j(\rho P_i) \right) \right) \\
& + \frac{4}{3}\pi D_R \ell_c^3 U_0 \rho^2 \left(\frac{2}{3} P_i - P_j N_{ij} \right), \tag{B.4}
\end{aligned}$$

$$\begin{aligned}
\dot{N}_{ij}^L = & -\nabla \cdot [(b_1 \mathbf{T}^1 + b_2 \mathbf{T}^2) \rho N_{ij}] \\
& - \frac{1}{5} b_3 \partial_z \left(T_{zj}^3 \rho P_i + T_{zi}^3 \rho P_j - \frac{2}{3} \delta_{ij} T_{zl}^3 \rho P_l \right) \\
& + \frac{\rho}{7} \left(\frac{7}{5} [b_1 (T_{ij}^4 + T_{ji}^4) - b_2 (T_{ij}^5 + T_{ji}^5)] + 5b_1 T_{il}^4 N_{jl} \right. \\
& - \frac{14}{15} b_1 T_{il}^4 \delta_{ij} - 2b_1 T_{li}^4 N_{lj} - 3b_2 T_{il}^5 N_{lj} - 2b_1 T_{lj}^4 N_{li} + 5b_1 T_{jl}^4 N_{li} \\
& \left. - 3b_2 T_{ij}^5 N_{li} - 2b_1 T_{il}^4 N_{ij} - 2 [b_1 T_{ml}^4 - b_2 T_{ml}^5] N_{ml} \delta_{ij} \right) \\
& + \frac{4}{315} b_4 \rho \left(-9T_{li}^6 P_j + 26T_{ijl}^6 P_l - 9T_{lj}^6 P_i - 9T_{ilm}^6 P_m \delta_{ij} \right. \\
& \left. + 26T_{jil}^6 P_l - 9T_{lij}^6 P_l \right). \tag{B.5}
\end{aligned}$$

$$\begin{aligned}
\dot{N}_{ij}^S = & -\frac{4}{3}\pi\ell_c^3 U_0 \partial_k \left(\rho \left(\frac{1}{35} D_2 \left(\partial_l(\rho P_l) P_i \delta_{jk} + \partial_l(\rho P_l) P_j \delta_{ik} \right. \right. \right. \\
& - \frac{4}{3} (\partial_l(\rho P_l) P_k + \partial_l(\rho P_k) P_l) \delta_{ij} + \partial_l(\rho P_i) P_l \delta_{jk} \\
& + \partial_l(\rho P_j) P_l \delta_{ik} + \partial_i(\rho P_m) P_m \delta_{jk} + \partial_j(\rho P_m) P_m \delta_{ik} \\
& \left. \left. \left. + (\partial_j(\rho P_i) + \partial_i(\rho P_j)) P_k + \partial_j(\rho P_k) P_i + \partial_i(\rho P_k) P_j \right) \right) \right) \\
& - \frac{2}{21} D_5 \partial_k(\rho P_l) P_l \delta_{ij} + \frac{1}{5} D_4 \partial_k [(\rho P_i) P_j + (\rho P_j) P_i] \Big) \\
& + \frac{8}{5}\pi D_R \ell_c^3 U_0 \rho^2 \left(P_i P_j - \frac{P^2}{3} \delta_{ij} \right). \tag{B.6}
\end{aligned}$$

In sections 4.2 and 4.3 where, we studied the linear stability of isotropic and polar phases we needed to linearize the interaction contributions. Here we briefly present the details of such calculations for a typical term. Let us consider the first term of $\dot{\rho}^L$ in density equation (B.1). We have:

$$-b_1 \partial_i (T_i^1 \rho) = -b_1 \partial_i \left(\int d\mathbf{r}' \frac{\hat{R}_i}{R^2} M_{jk}(\hat{\mathbf{R}}) \rho(\mathbf{r}') N_{jk}(\mathbf{r}') \rho(\mathbf{r}) \right), \tag{B.7}$$

where $\mathbf{R} = \mathbf{r} - \mathbf{r}'$. Now we can substitute isotropic values of ρ and \mathbf{N} from (67) and (69) to (B.7). Taking the spatial Fourier transform and defining $W_{ijk} = \frac{\hat{k}_i}{R^2} M_{jk}$, we will have:

$$\begin{aligned} -b_1 \partial_i (T_i^1 \rho) &= -b_1 \rho_0^2 \partial_i \left(\int d\mathbf{r}' \int d\mathbf{k} e^{-i\mathbf{k} \cdot (\mathbf{r} - \mathbf{r}')} \check{W}_{ijk}(\mathbf{k}) \int d\mathbf{k}' e^{-i\mathbf{k}' \cdot \mathbf{r}'} \delta \check{N}_{jk}(\mathbf{k}') \right) \\ &= -b_1 \rho_0^2 \partial_i \left(\int d\mathbf{k} \int d\mathbf{k}' \delta(\mathbf{k} - \mathbf{k}') \check{W}_{ijk}(\mathbf{k}) e^{-i\mathbf{k} \cdot \mathbf{r}} \delta \check{N}_{jk}(\mathbf{k}') \right) \\ &= i b_1 \rho_0^2 \left(\int d\mathbf{k} e^{-i\mathbf{k} \cdot \mathbf{r}} k_i \check{W}_{ijk}(\mathbf{k}) \delta \check{N}_{jk}(\mathbf{k}) \right). \end{aligned} \quad (\text{B.8})$$

To proceed further, we need to calculate the Fourier transform of W_{ijk} . As a result of symmetry, the following general expression for \check{W}_{ijk} can be written:

$$\check{W}_{ijk} = A \hat{k}_i \hat{k}_j \hat{k}_k + B \hat{k}_i \delta_{jk} + C \hat{k}_j \delta_{ik} + D \hat{k}_k \delta_{ij}, \quad (\text{B.9})$$

where scalar functions A , B , C and D can depend on k and Fourier transform is defined by:

$$\check{W}_{ijk} = \int d\mathbf{R} e^{i\mathbf{k} \cdot \mathbf{R}} W_{ijk}(\mathbf{R}). \quad (\text{B.10})$$

Multiplying the above two equations by $\hat{k}_i \hat{k}_j \hat{k}_k$, $\hat{k}_i \delta_{jk}$, $\hat{k}_j \delta_{ik}$ and $\hat{k}_k \delta_{ij}$ respectively, we will obtain the following four equations for unknown functions:

$$A + B + C + D = \int d\mathbf{R} e^{i\mathbf{k} \cdot \mathbf{R}} \frac{1}{R^2} \left((\hat{\mathbf{k}} \cdot \hat{\mathbf{R}})^3 - \frac{1}{3} (\hat{\mathbf{k}} \cdot \hat{\mathbf{R}}) \right), \quad (\text{B.11})$$

$$A + 3B + C + D = 0, \quad (\text{B.12})$$

$$A + B + 3C + D = \frac{2}{3} \int d\mathbf{R} e^{i\mathbf{k} \cdot \mathbf{R}} \frac{1}{R^2} (\hat{\mathbf{k}} \cdot \hat{\mathbf{R}}), \quad (\text{B.13})$$

$$A + B + C + 3D = \frac{2}{3} \int d\mathbf{R} e^{i\mathbf{k} \cdot \mathbf{R}} \frac{1}{R^2} (\hat{\mathbf{k}} \cdot \hat{\mathbf{R}}). \quad (\text{B.14})$$

By evaluating the integrals, we can obtain the following result for \check{W}_{ijk} :

$$\check{W}_{ijk} = -\frac{8\pi i}{3k} \hat{k}_i \hat{k}_j \hat{k}_k + \frac{4\pi i}{3k} \hat{k}_j \delta_{ik} + \frac{4\pi i}{3k} \hat{k}_k \delta_{ij}. \quad (\text{B.15})$$

With a similar procedure, all other interaction integrals can be calculated.

References

- [1] J Toner, Y Tu, and S Ramaswamy. Hydrodynamics and phases of flocks. *Annals of Physics*, 318:170–244, 2005.
- [2] M C Marchetti, J F Joanny, S Ramaswamy, T B Liverpool, J Prost, M Rao, and R A Simha. Hydrodynamics of soft active matter. *Reviews of Modern Physics*, 85:1143, 2013.
- [3] T Vicsek and A Zafeiris. Collective motion. *Physics Reports*, 517:71–140, 2012.
- [4] S Ramaswamy. Active matter. *Journal of Statistical Mechanics: Theory and Experiment*, 2017:054002, 2017.

- [5] Ch Becco, N Vandewalle, J Delcourt, and P Poncin. Experimental evidences of a structural and dynamical transition in fish school. *Physica A: Statistical Mechanics and its Applications*, 367:487–493, 2006.
- [6] A Cavagna, L Del Castello, I Giardina, T Grigera, A Jelic, S Melillo, T Mora, L Parisi, E Silvestri, M Viale, and A M Walczak. Flocking and turning: a new model for self-organized collective motion. *Journal of Statistical Physics*, 158:601–627, 2015.
- [7] M Nagy, Z Akos, D Biro, and T Vicsek. Hierarchical group dynamics in pigeon flocks. *Nature*, 464:890–893, 2010.
- [8] F Peruani, J Starruß, V Jakovljevic, L Søgaard-Andersen, A Deutsch, and M Bär. Collective motion and nonequilibrium cluster formation in colonies of gliding bacteria. *Physical Review Letters*, 108:098102, 2012.
- [9] R Tokita, T Katoh, Y Maeda, J-i Wakita, M Sano, T Matsuyama, and M Matsushita. Pattern formation of bacterial colonies by escherichia coli. *Journal of the Physical Society of Japan*, 78:074005, 2009.
- [10] E Lushi, H Wioland, and R E Goldstein. Fluid flows created by swimming bacteria drive self-organization in confined suspensions. *Proceedings of the National Academy of Sciences*, 111:9733–9738, 2014.
- [11] A Sokolov, I S Aranson, J O Kessler, and R E Goldstein. Concentration dependence of the collective dynamics of swimming bacteria. *Physical Review Letters*, 98:158102, 2007.
- [12] J Prost, F Jülicher, and JF Joanny. Active gel physics. *Nature Physics*, 11:111–117, 2015.
- [13] I Theurkauff, C Cottin-Bizonne, J Palacci, C Ybert, and L Bocquet. Dynamic clustering in active colloidal suspensions with chemical signaling. *Physical Review Letters*, 108:268303, 2012.
- [14] I Buttinoni, J Bialké, F Kümmel, H Löwen, C Bechinger, and T Speck. Dynamical clustering and phase separation in suspensions of self-propelled colloidal particles. *Physical Review Letters*, 110:238301, 2013.
- [15] P Bayati and A Najafi. Dynamics of two interacting active janus particles. *Journal of Chemical Physics*, 144:134901, 2016.
- [16] V Narayan, S Ramaswamy, and N Menon. Long-lived giant number fluctuations in a swarming granular nematic. *Science*, 317:105–108, 2007.
- [17] V Schaller, C Weber, C Semmrich, E Frey, and A R Bausch. Polar patterns of driven filaments. *Nature*, 467:73–77, 2010.
- [18] Y Sumino, K H Nagai, Y Shitaka, D Tanaka, K Yoshikawa, H Chaté, and K Oiwa. Large-scale vortex lattice emerging from collectively moving microtubules. *Nature*, 483:448–452, 2012.
- [19] N D Mermin and H Wagner. Absence of ferromagnetism or antiferromagnetism in one or two-dimensional isotropic heisenberg models. *Physical review letters*, 17:1133, 1966.
- [20] J Toner and Y Tu. Long-range order in a two-dimensional dynamical xy model: How birds fly together. *Physical Review Letters*, 75:4326, 1995.
- [21] A Baskaran and M C Marchetti. Statistical mechanics and hydrodynamics of bacterial suspensions. *Proceedings of the National Academy of Sciences*, 106:15567, 2009.
- [22] J Blaschke, M Maurer, K Menon, A Zöttl, and H Stark. Phase separation and coexistence of hydrodynamically interacting microswimmers. *Soft matter*, 12:9821–9831, 2016.
- [23] D Saintillan and M J Shelley. Instabilities and pattern formation in active particle suspensions: kinetic theory and continuum simulations. *Physical Review Letters*, 100:178103, 2008.
- [24] H Behmadi, Z Fazli, and A Najafi. A 2d suspension of active agents: the role of fluid mediated interaction. *Journal of Physics: Condensed Matter*, 29:115102, 2017.
- [25] D Saintillan and M J Shelley. Instabilities, pattern formation, and mixing in active suspensions. *Physics of Fluids*, 20:123304, 2008.
- [26] C A Whitfield, T C Adhyapak, A Tiribocchi, G P Alexander, D Marenduzzo, and S Ramaswamy. Hydrodynamic instabilities in active cholesteric liquid crystals. *The European Physical Journal E*, 40:50, 2017.
- [27] N Oyama, J J Molina, and R Yamamoto. Simulations of model microswimmers with fully resolved

- hydrodynamics. *Journal of the Physical Society of Japan*, 86:101008, 2017.
- [28] M M Genkin, A Sokolov, O D Lavrentovich, and I S Aranson. Topological defects in a living nematic ensnare swimming bacteria. *Physical Review X*, 7:011029, 2017.
- [29] S Ramaswamy and M Rao. Active-lament hydrodynamics: instabilities, boundary conditions and rheology. *New Journal of Physics*, 9:423, 2007.
- [30] A Zöttl and H Stark. Hydrodynamics determines collective motion and phase behavior of active colloids in quasi-two-dimensional confinement. *Physical Review Letters*, 112:118101, 2014.
- [31] F Peruani, A Deutsch, and M Bär. Nonequilibrium clustering of self-propelled rods. *Physical Review E*, 74:030904, 2006.
- [32] T Vicsek, A Czirók, E Ben-Jacob, I Cohen, and O Shochet. Novel type of phase transition in a system of self-driven particles. *Physical review letters*, 75:1226, 1995.
- [33] H Chaté, F Ginelli, G Grégoire, F Peruani, and F Raynaud. Modeling collective motion: variations on the vicsek model. *The European Physical Journal B*, 64:451–456, 2008.
- [34] A Baskaran and M C Marchetti. Enhanced diffusion and ordering of self-propelled rods. *Physical Review Letters*, 101:268101, 2008.
- [35] J Toner and Y Tu. Flocks, herds, and schools: A quantitative theory of flocking. *Physical Review E*, 58:4828, 1998.
- [36] S Ramaswamy and R A Simha. Hydrodynamic fluctuations and instabilities in ordered suspensions of self-propelled particles. *Physical Review Letters*, 89:058101, 2002.
- [37] S Mishra, A Baskaran, and M C Marchetti. Fluctuations and pattern formation in self-propelled particles. *Physical Review E*, 81:061916, 2010.
- [38] E Bertin, M Droz, and G Grégoire. Hydrodynamic equations for self-propelled particles: microscopic derivation and stability analysis. *Journal of Physics A: Mathematical and Theoretical*, 42:445001, 2009.
- [39] E M Purcell. Life at low reynolds number. *American Journal of Physics*, 45:3–11, 1977.
- [40] A Najafi and R Golestanian. Propulsion at low reynolds number. *Journal of Physics: Condensed Matter*, 17:S1203, 2005.
- [41] R Zargar, A Najafi, and MF Miri. Three-sphere low-reynolds-number swimmer near a wall. *Physical Review E*, 80:026308, 2009.
- [42] C Pozrikidis. *Boundary integral and singularity methods for linearized viscous flow*. Cambridge University Press, 1992.
- [43] M Moradi and A Najafi. Rheological properties of a dilute suspension of self-propelled particles. *Europhysics Letters*, 109:24001, 2015.
- [44] M Farzin, K Ronasi, and A Najafi. General aspects of hydrodynamic interactions between three-sphere low reynolds number swimmers. *Physical Review E*, 85:061914, 2012.
- [45] G P Alexander, C M Pooley, and J M Yeomans. Hydrodynamics of linked sphere model swimmers. *Journal of Physics: Condensed Matter*, 21:204108, 2009.
- [46] E Lauga and T R Powers. The hydrodynamics of swimming microorganisms. *Reports on Progress in Physics*, 72:096601, 2009.
- [47] J Elgeti, R G Winkler, and G Gompper. Physics of microswimmers: single particle motion and collective behavior: a review. *Reports on Progress in Physics*, 78:056601, 2015.
- [48] K Drescher, R E Goldstein, N Michel, M Polin, and I Tuval. Direct measurement of the flow field around swimming microorganisms. *Physical Review Letters*, 105:168101, 2010.
- [49] A Najafi and R Golestanian. Coherent hydrodynamic coupling for stochastic swimmers. *Europhysics Letters*, 90:68003, 2010.
- [50] S Kim and S J Karrila. *Microhydrodynamics Principles and Selected Applications*. Dover Publications, Inc., New York, 2005.
- [51] J Happel and H Brenner. *Low Reynolds Number Hydrodynamics with special applications to particulate media*. Prentice-Hall, Englewood Cliffs, NJ, 1965.
- [52] N Yoshinaga and T B Liverpool. Hydrodynamic interactions in dense active suspensions: From polar order to dynamical clusters. *Physical Review E*, 96:020603, 2017.

- [53] J R Howse, R A L Jones, A J Ryan, T Gough, R Vafabakhsh, and R Golestanian. Self-motile colloidal particles: From directed propulsion to random walk. *Physical Review Letters*, 99:048102, 2007.
- [54] A Baskaran and M C Marchetti. Hydrodynamics of self-propelled hard rods. *Physical Review E*, 77(6):011920, 2008.